

Revelo et al., <http://www.jcb.org/cgi/content/full/jcb.201402066/DC1>

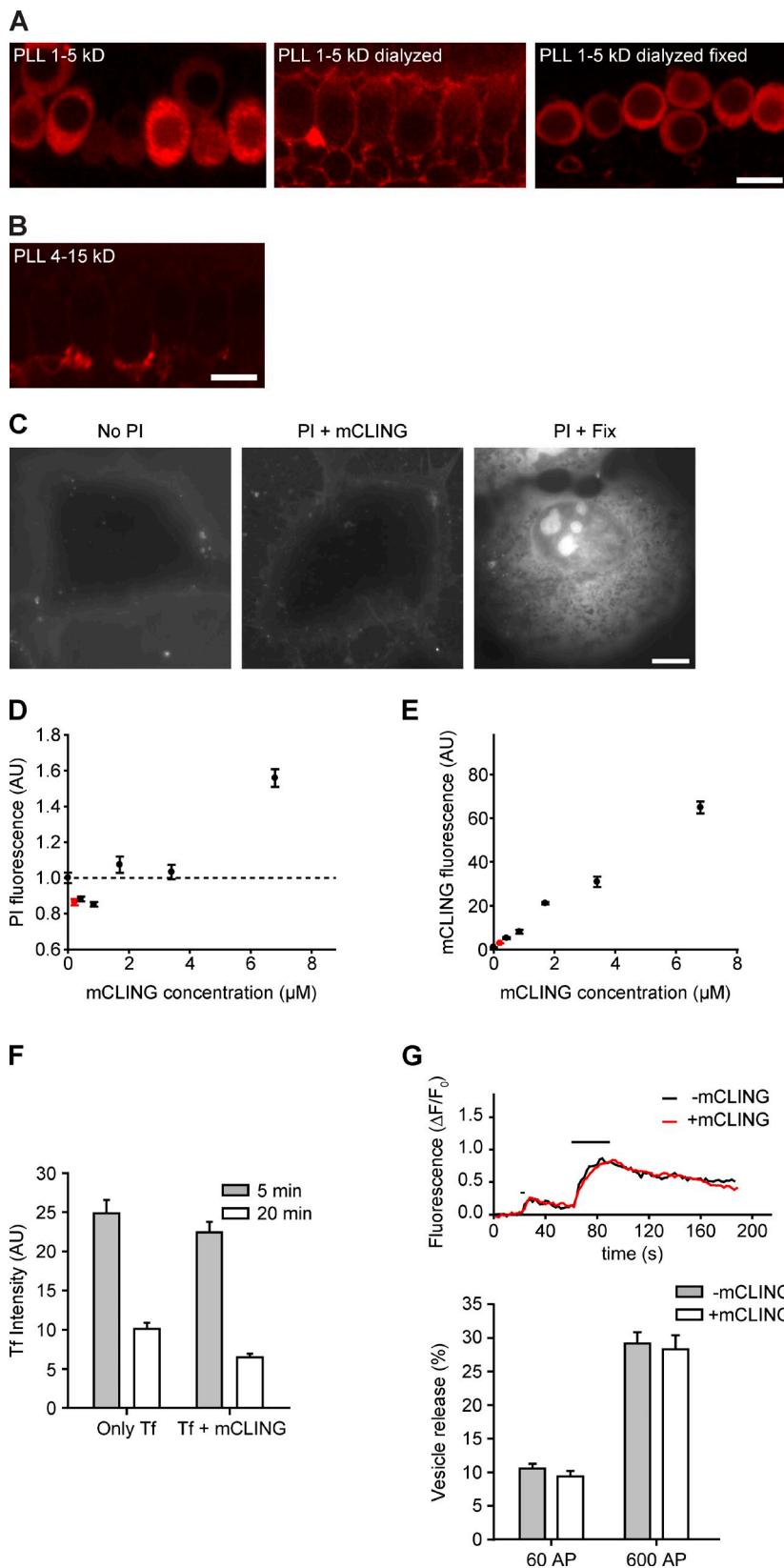
Figure S1. Testing membrane-binding probes in the

organ of Corti and in cultured cells. (A and B) Size requirements for a successful endocytosis marker in IHCs.

(A) Commercial poly-L-lysine (PLL) in the range of 1–5 kD was conjugated to Atto647N. (left) The molecules labeled living IHCs in a way similar to FM 1-43 (Fig. 1 D, insets), probably as a result of penetration of small PLLs (<1 kD) still present in the mixture through the mechanotransducer channels. (middle) After dialysis of the Atto647N-PLL mixture against a 3.5-kD selection membrane, penetration inside IHCs was strongly reduced. (right) However, these labels disengaged from membranes upon fixation and/or permeabilization and were again found throughout the cells. (B) Atto647N-labeled PLL molecules of sizes between 4 and 15 kD are too large to penetrate efficiently into the organ of Corti.

(C–G) mCLING does not have toxic effects. We incubated COS7 cells with propidium iodide (PI), in the presence of different amounts of mCLING. (C) The propidium iodide fluorescence of a cell treated with mCLING (center) is compared with that of a fixed cell (right) or a cell not treated with propidium iodide (left). mCLING does not cause any propidium iodide entry into the cells. (D) Quantification of the propidium iodide fluorescence normalized to the control treatment (no mCLING), as a function of mCLING concentration. The dotted line indicates the propidium iodide fluorescence level in the control treatment. Propidium iodide fluorescence only increases above the cellular autofluorescence when mCLING surpasses 5  $\mu$ M. The red dot indicates the concentration of mCLING we used in cellular experiments (0.4  $\mu$ M).

(E) Plot of mCLING fluorescence, in the same experiment. (F) Quantification of transferrin uptake and traffic-dependent release from mCLING-treated cells. COS7 cells were incubated with Alexa Fluor 546–transferrin (Tf) for 5 min at 37°C and were then washed and incubated in its absence for a further 20 min at 37°C to measure the release of transferrin. Note that both transferrin uptake and release are normal in presence of mCLING, when compared with control cells. Error bars represent mean fluorescence intensity  $\pm$  SEM for 40–44 cells per condition. (G) Quantification of synaptic vesicle recycling in the presence of mCLING. Cultured hippocampal neurons were transfected with synaptophysin (Miesenböck et al., 1998; Sankaranarayanan and Ryan, 2000) and were then stimulated at 20 Hz for 3 s (60 action potentials [AP]) followed by a longer stimulus (30 s, 600 action potentials) after an interval of 40 s. The onset and the length of the stimuli are indicated by black horizontal bars. Exocytosis causes increases in the synaptophysin fluorescence. These are followed by decreases in fluorescence, which correspond to endocytosis (top graph, representative traces from one mCLING-treated and one untreated neuron are shown; the traces are typical for five and six independent experiments, respectively). In the bottom graph, we investigated the amount of exocytosis caused by the two stimuli, expressed as percentage of all vesicles (after normalizing the synaptophysin fluorescence changes induced by the stimuli to the entire amount of synaptophysin, measured after an ammonium chloride pulse). (bottom) The values are virtually identical in mCLING-treated and control neurons. Error bars represent mean percentages  $\pm$  SEM. Control neurons: six experiments and 138 boutons analyzed. mCLING treated neurons: five experiments and 103 boutons analyzed. AU, arbitrary unit. Bars, 10  $\mu$ m.



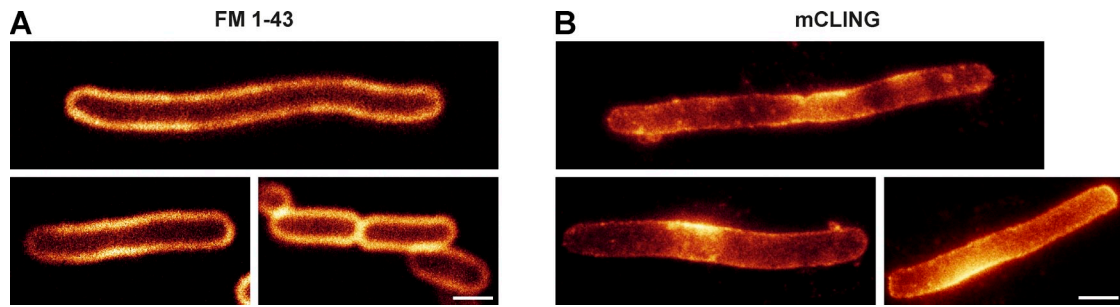


Figure S2. **Imaging of *E. coli* using FM 1-43 or mCLING.** (A) *E. coli* bacteria were incubated with FM 1-43 for 5 min followed by imaging in PBS using a confocal microscope. (B) The cells were incubated with mCLING in the same fashion as with FM 1-43 and were imaged using STED microscopy. Note the higher resolution of the images. The membrane of the bacteria is not homogeneously labeled, either for FM 1-43 or for mCLING. Central regions often appear brighter than other regions. The biological relevance of this phenomenon, which is more visible with mCLING, remains to be investigated. Bars, 1  $\mu$ M.

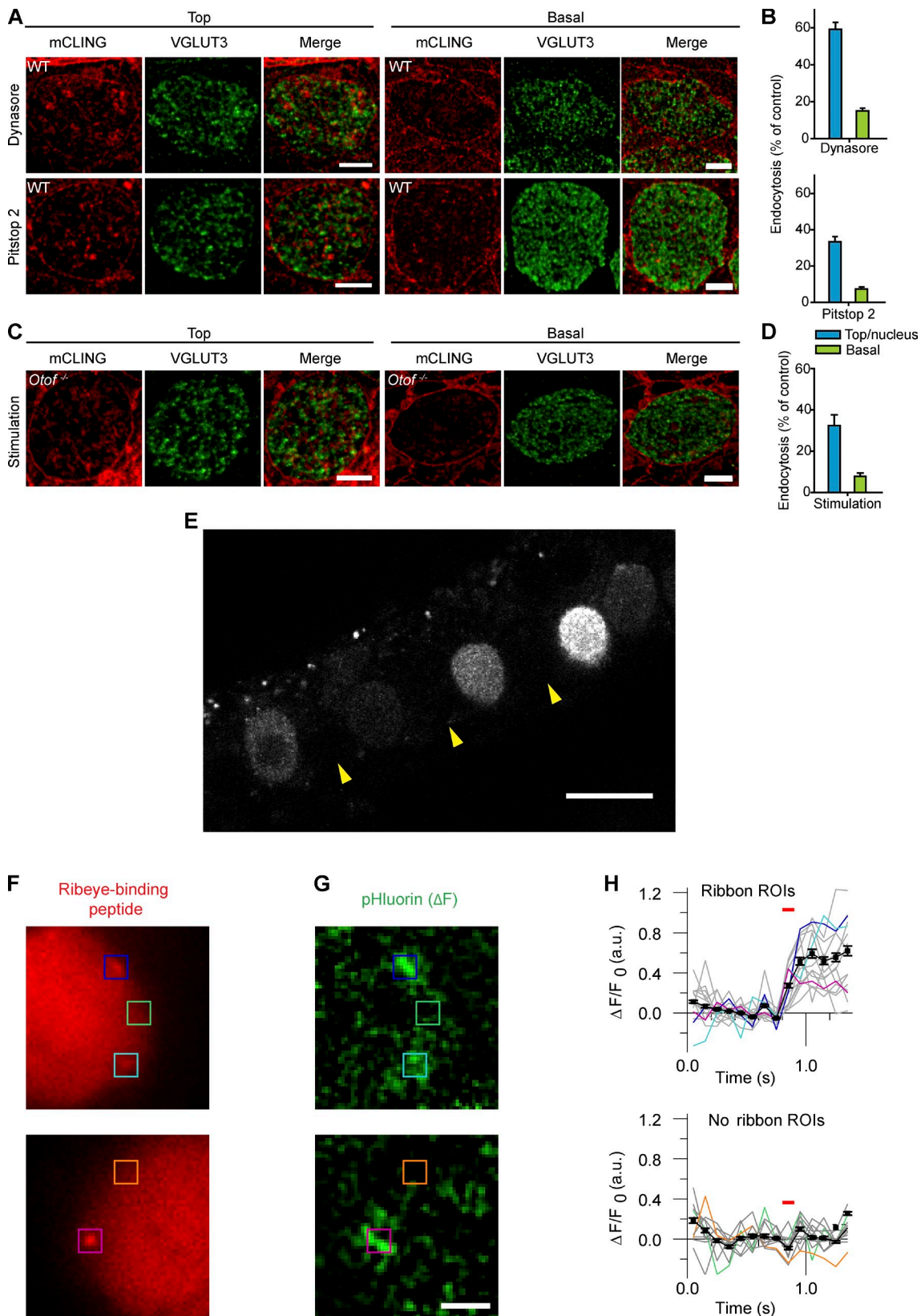


Figure S3. **Measurements of synaptic vesicle recycling in IHCs by mCLING under inhibition of endocytosis and by a pH-sensitive GFP variant.** (A and B) Effects of treatments that impair endo- or exocytosis in IHCs. mCLING uptake is reduced by clathrin and dynamin inhibitors. (A) IHCs were incubated with the dynamin inhibitor dynasore (100  $\mu$ M) or, alternatively, with the clathrin inhibitor pitstop 2 (30  $\mu$ M) for 25 min, and were then stimulated using 65 mM KCl for 1 min in buffer containing mCLING. (B) The amount of mCLING endocytosis at the top/nuclear and basal levels was compared with the corresponding values in control wild-type cells (see examples in Fig. 4 C). Both drugs reduce endocytosis in the vicinity of release sites to almost negligible levels, whereas they allow more endocytosis elsewhere. The error bars indicate the mCLING uptake in dynasore and pitstop 2-treated cells as percentages of the

control. Error bars represent mean percentages  $\pm$  SEM from 54 cell tops and 100 cell bases treated with dynasore and 63 cell tops and 52 cell bases treated with pitstop 2. (C and D) Impaired synaptic vesicle exocytosis leads to reduced mCLING uptake in the IHC. (C) IHCs from otoferlin-deficient animals (*Otof*<sup>-/-</sup>), in which exocytosis is completely abolished, were stimulated in the presence of mCLING. Endocytosis was reduced, especially at the base of the cell. (D) As for B, the amount of endocytosis was compared with that in control cells (see examples in Fig. 4 C). Error bars represent mean percentages  $\pm$  SEM from 28 cell tops and 26 cell bases. The treatment with endocytosis inhibitors was performed as follows. After a 5-min incubation in HBSS without Ca<sup>2+</sup>, the organs were incubated for 25 min in a solution of 30  $\mu$ M pitstop 2 (ab120687; Abcam) or 100  $\mu$ M dynasore (D7693; Sigma-Aldrich), diluted in HBSS without Ca<sup>2+</sup>. The organs were then incubated for 2 min in mCLING-containing HBSS without Ca<sup>2+</sup> + inhibitor (same concentration) and were then stimulated for 1 min in HBSS high K<sup>+</sup> + 1.7  $\mu$ M mCLING + inhibitor (same concentrations). The entire process was performed at 37°C in a closed 12-well plate continuously supplied with carbogen to keep pH levels stable. Fixation, quenching, and immunostaining were performed as described for mCLING labeling and immunostaining. (E–H) Synaptic vesicles are released close to the synaptic ribbon in IHCs. (E) Live confocal image of an organ of Corti after embryonic injection of VGLUT1-pHluorin virus, showing the resting fluorescence of a stretch of transduced and nontransduced (yellow arrowheads) IHCs. Expression level of VGLUT1-pHluorin also varied among transduced IHCs. (F) Live confocal images of a TAMRA-conjugated Ribeye-binding peptide introduced into IHCs through patch pipette, which marked the location of synaptic ribbons (blue, cyan, and magenta boxes; Zenisek et al., 2004). Extrasynaptic regions were selected for comparison (orange and green boxes). (G) Change in VGLUT1-pHluorin fluorescence in IHCs shown in B upon depolarizing to  $-17$  mV for 100 ms. Baseline fluorescence (average of five frames at 10 Hz) before depolarization was subtracted from fluorescence after depolarization (averaged of five frames at 10 Hz). The image was further smoothed with a 2D Gaussian kernel (120-nm width) for display. (H) Individual (gray and colored) and average (black;  $\pm$ SEM) baseline-normalized fluorescence intensity change ( $\Delta F/F_0$ ) of 16 active zone (top) and 10 nonactive zone regions (bottom) in nine IHCs from six injected ears as the function of time, each obtained from a square region of interest (ROI; 920  $\times$  920 nm) either centered at a synaptic ribbon or cell border identified through the background fluorescence of the peptide. Colored traces represent the fluorescence intensities of the ROIs marked in F and G. Red bar marks the duration of depolarization. Note the rise in pHluorin signal at active zones (ribbon ROIs) but not in nonactive zone regions (no ribbon ROIs) upon stimulation. The data presented in the figure are representative of six independent viral transductions (injections). a.u., arbitrary unit. Bars: (A, C, F, and G) 2  $\mu$ m; (E) 15  $\mu$ m.

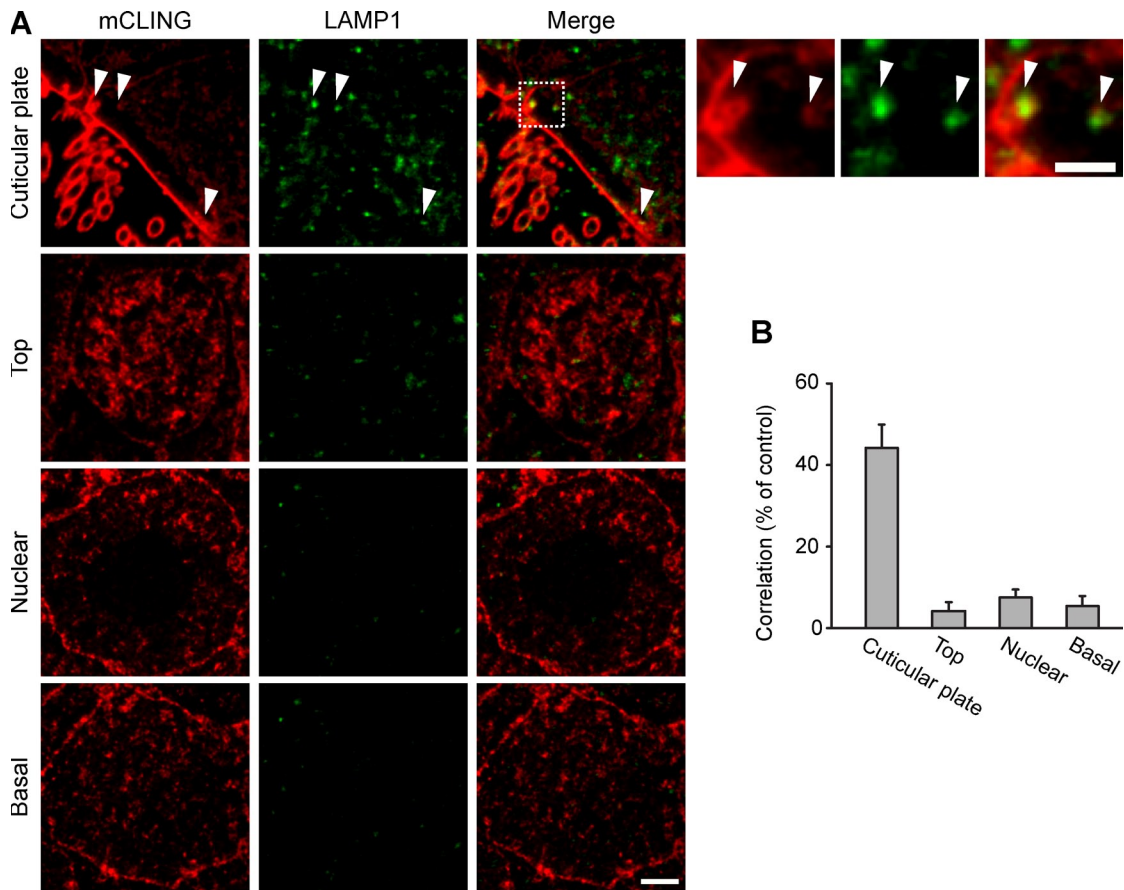


Figure S4. **Analysis of apical endocytosis in IHCs.** (A) IHCs were labeled with mCLING as in Fig. 4 C and were immunostained for the late endosome/lysosome marker LAMP1. A few labeled organelles can be observed in the apical region of the cell, at the level of the cuticular plate. Several colocalize with LAMP1 (arrowheads). LAMP1 is not abundant in the rest of the cell and does not correlate well with other mCLING-labeled organelles. Boxed area is magnified on the right. Bars: (main images) 1  $\mu\text{m}$ ; (magnifications) 0.5  $\mu\text{m}$ . (B) Pearson's correlation coefficients were determined as in Fig. 6. Note the correlation at the level of the cuticular plate. 125–403 organelles were analyzed for each cellular region from two independent experiments. Error bars show SEMs.

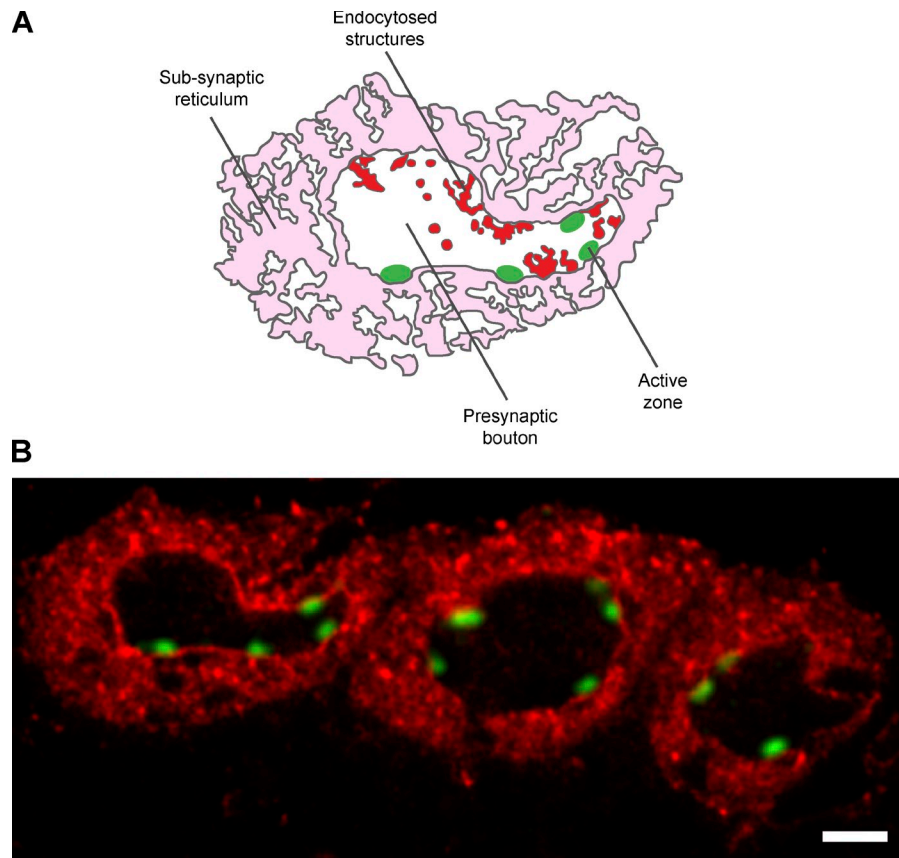


Figure S5. **mCLING use in *Drosophila*.** (A) Model of the *Drosophila* larva neuromuscular junction. (B) A neuromuscular junction was stimulated in presence of mCLING, was fixed and immunostained for the active zone protein Bruchpilot, using the nc82 antibody (Developmental Studies Hybridoma Bank). Note the presence of mCLING staining within the synapse, representing endocytosis, as in IHCs. Bar, 1  $\mu$ m.

## References

- Miesenböck, G., D.A. De Angelis, and J.E. Rothman. 1998. Visualizing secretion and synaptic transmission with pH-sensitive green fluorescent proteins. *Nature*. 394:192–195. <http://dx.doi.org/10.1038/28190>
- Sankaranarayanan, S., and T.A. Ryan. 2000. Real-time measurements of vesicle-SNARE recycling in synapses of the central nervous system. *Nat. Cell Biol.* 2:197–204.
- Zenisek, D., N.K. Horst, C. Merrifield, P. Sterling, and G. Matthews. 2004. Visualizing synaptic ribbons in the living cell. *J. Neurosci.* 24:9752–9759. <http://dx.doi.org/10.1523/JNEUROSCI.2886-04.2004>

**Zip file 1 contains the routine used to calculate the percentage of cellular area occupied by mCLING-labeled organelles.**

**Zip file 2 contains the routine used to calculate Pearson's correlation values between the mCLING and the immunostaining channels across mCLING-labeled organelles.**

**Zip file 3 contains the routine used to generate average pictures of aligned ribbon-type active zones and to generate average images of mCLING-labeled and immunostained synaptic vesicles. Instructions on how to use these macros can be found in the program\_start.m file of each folder.**